ISSN 1070-4272, Russian Journal of Applied Chemistry, 2009, Vol. 82, No. 3, pp. 343–351. © Pleiades Publishing, Ltd., 2009.
Original Russian Text © V.V. Sidorchuk, S.V. Khalameida, V.A. Zazhigalov, 2009, published in Zhurnal Prikladnoi Khimii, 2009, Vol. 82, No. 3, pp. 353–360.

INORGANIC SYNTHESIS AND INDUSTRIAL INORGANIC CHEMISTRY

Hydrothermal Deposition of Vanadium Phosphates onto Carbon Materials

V. V. Sidorchuk, S. V. Khalameida, and V. A. Zazhigalov

Institute of Sorption and Problems of Endoecology, National Academy of Sciences of Ukraine, Kiev, Ukraine

Received August 8, 2008

Abstract—Vanadium-phosphorus oxide compounds of various chemical and phase compositions were synthesized by hydrothermal and microwave techniques on the surface of carbon materials (activated carbons, nanotubes, graphite). The composites obtained were studied by means of X-ray phase and differential-thermal analyses, nitrogen adsorption, and scanning electron microscopy.

DOI: 10.1134/S107042720903001X

Recently, carbon materials of varied origin and structure have been widely used as catalyst supports [1–3], which is due to their advantages, such as the large specific surface area, developed (and controllable) porous structure, chemical stability in various media, and sufficiently high thermal stability and mechanical strength [3, 4]. A disadvantage of carbon supports, the low concentration of functional groups on the surface and the resulting low degree of deposition of the active component [5], is overcome by oxidation of activated carbons and other materials [3, 4, 6]. Vanadium phosphates are used as catalysts for some processes of mild oxidation of hyd-rocarbons, ion exchangers, and cathode materials for lithium power cells [2, 7–10]. However, these com-pounds, as a rule, have a small specific surface area and a weakly developed porosity. Therefore, their effective use frequently requires their deposition onto the surface of supports.

Previously, results obtained in deposition of vanadium-phosphorus oxide (VPO) catalysts [specifically, vanadyl hydrophosphate (VHP)] onto silica-carbon supports (carbosils) having a layer of pyrolytic carbon on their surface were reported [11]. However, supports of this kind have a thermal stability insufficient for the use of supported catalysts in some oxidative processes.

The aim of this study was to examine deposition processes of the VPO phase onto the surface of pure carbon materials by both hydrothermal treatment (HTT) with both the ordinary convective heating and microwave heating (MWT) and to analyze some physicochemical properties of the composites obtained. It should be noted that bulk VPO catalysts have been synthesized previously by HTT and MWT [7, 12–14]. No reports of deposition of vanadium-phosphorus oxide phases onto the surface of pure carbon supports by the hydrothermal and microwave methods were found in the literature.

EXPERIMENTAL

The following carbon materials were used as supports: activated kernel carbons with varied porous structure [KAU (Ukraine)]; A2PS and PS-3 (Poland); carbon nanotubes (C-NT) synthesized by pyrolysis of ethylene, nonporous (unwashed) and porous (washed to remove metals catalyzing the synthesis of C-NT proper); and nonporous graphite powder. All of the chosen supports were used both in the initial state and after a hydrothermal oxidation with hydrogen peroxide, which led to a pronounced increase in the amount of oxygen-containing groups on the surface [16]. The supports were subjected to preliminary oxidation in the vapor phase by HTT and MWT with

Table 1. Pores structure parameters of unoxidized and oxidized carbon supports

Material	Oxidation conditions	S_{BET}, m^2 g^{-1}	S_{m_i}, m^2 g^{-1}	V_{N_2}, cm^3 g^{-1}	V_{m_i}, cm^3 g^{-1}	V_{m_e}, cm^3 g^{-1}
A2PS	Unoxidized	1054	930	0.94	0.47	0.46
	HTT 200°C 30% H_2O_2	1239	402	0.70	0.18	0.46
	MWT 200°C 30% H_2O_2	1394	616	0.78	0.27	0.49
PS-3	Unoxidized	1545	867	1.00	0.72	0.30
	HTT 200°C 30% H_2O_2	1808	740	1.02	0.60	0.32
KAU	Unoxidized	952	796	0.51	0.33	0.15
	HTT 350°C 30% H_2O_2	973	662	0.54	0.28	0.26
	Double HTT 170°C 30% H_2O_2	725	436	0.46	0.21	0.26
	HTT 170°C 50% H_2O_2	706	336	0.39	0.15	0.24
Nonporous C-NT	Unoxidized	195	–	–	–	–
	HTT 200°C 30% H_2O_2	125	2.65	–	–	–
Porous C-NT	Unoxidized	260	29	1.00	0.015	0.95
Graphite	Unoxidized	16	–	–	–	–

30 and 50% aqueous solutions of H_2O_2. The pores structure parameters of the supports are listed in Table 1. The reaction mixture used for deposition had the following composition: (1) 0.8 g of crystalline V_2O_5, 10 ml of distilled water, 85% H_3PO_4 in an amount corresponding to synthesis of VHP in a 15% excess ($P/V = 1.15$), and 5 g of the carbon material; the V_2O_5/support ratio in the mixture was chosen so as to deposit 30 wt % VHP phase onto the carbon surface (it is known that VHP is a precursor of the catalytically active phase in oxidation reactions; at the same time, VHP as an acid salt is a typical ion-exchange material [8]; (2) 10 ml of an aqueous solution of ammonium meta-vanadate (saturated at 90°C, 0.3 M solution), H_3PO_4, and 5 g of a carbon material. All the substances used were of chemically pure grade.

The vapor-phase oxidation of the carbons and the liquid-phase reaction of VPO deposition were performed in a laboratory autoclave with quartz inserts (HTT) or in a NANO-2000 microwave reactor (Plazmotronica, Poland) (MWT). The oxidation temperature was 170 or 200°C. KAU was oxidized under more severe conditions: in the autoclave at 350°C in 50% H_2O_2 and also by double HTT in 30% H_2O_2. The oxidation time was 3 h for HTT and 1 h for MWT. The VPO phase was deposited at 150–175°C in the course of 6 h in HTT and 1 h in MWT, after which the solid phase was washed with distilled water by decantation and the unreacted substances (and also part of products unbound to the support) were removed with washing water. The content of the supported VPO phase was found from the gain in mass as the weight difference between the weighed portion of a pure support and that after performing the reaction and washing. Preliminarily (prior to weighing), the support and the deposited sample were dried at 150°C for 3 h. For comparison, the amount of the VPO phase deposited onto the surface of the carbon host was calculated using thermogravimetric data, from the amount of carbon burnt at temperatures of up to 900°C.

An X-ray phase analysis (XPA) was performed on a Philips PW 1830 diffractometer (CuK_α radiation) under invariable measurement conditions. The X-ray diffraction patterns obtained were used to calculate the interplanar spacings and to estimate the absolute intensities of the principal reflections, which enabled comparison of the degrees of crystallinity of a set of samples. The crystallite size was determined using the Debye–Scherrer formula. The thermogravimetric analysis was performed with an MOM derivatograph-

Table 2. Synthesis conditions and the content of the supported phase

Support	Synthesis conditions		VPO content, wt %		T	ΔT, °C
	MWT, HTT	T, °C	gain in mass	DTA–TG		
Unoxidized A2PS	MWT	150	14.1	14.6	385	385–600
	MWT	175	24.2	25.9	380	380–610
	MWT[a]	175	10.4		420	420–830
	HTT	150	14.1	13.8	360	360–590
	HTT	175	22.9	23.9	380	380–640
	HTT[a]	175	9.3	–	–	–
Oxidized A2PS	MWT	175	28.5	30.2	380	380-600
	MWT[a]	175	14.0	–	480	480-830
	HTT	175	25.5	–	–	–
	HTT[a]	175	13.1	–	–	–
Unoxidized PS-3	MWT	175	21.7	25.7	390	390–600
	HTT	175	22.1	24.6	385	385–595
Oxidized PS-3	MWT	175	30.5	33.5	410	410–600
	HTT	175	27.5	31.9	400	400–560
Unoxidized KAU	HTT	175	16.4	15.5	360	360–620
Oxidized KAU, 350°C 30% H_2O_2	HTT	175	19.3	20.6	380	380–650
Twice oxidized KAU,350°C 30% H_2O_2	One HTT		20.3	21.5	380	380–620
	Two HTT		25.4	–	390	390–680
Oxidized KAU, 350°C 50% H_2O_2	HTT		23.2	–	385	385–670
Unoxidized graphite	MWT		9.2	9.5	460	460–720
	MWT		10.9	10.5	460	460–735
Oxidized graphite, 200°C 50% H_2O_2	MWT		12.6	12.3	465	465–750

[a] Synthesis from NH_4VO_3; in other cases, from V_2O_5.

C (Hungary) in air in the temperature range 20–1000°C at a heating rate of 10 deg min^{-1}.

The pores structure parameters of all the samples were calculated from nitrogen adsorption–desorption isotherms obtained with a Micromeritics ASAP 2405N analyzer; the specific surface area S_{BET} and the limiting-sorption pore volume V_{N_2}, from the amount of adsorption at a relative pressure close to unity; micropore surface area and volume, Smi and V_{m_i}, by the t-method; and the size distribution of mesopores, V_{m_e}, by the Barrett–Joyner–Halenda (BJH) method [17]. The total pore volume V_Σ was found by impregnation with water from the liquid phase. The surface morphology of the supported samples was studied by scanning electron microscopy (SEM) on a Tesla BS 301 instrument (Czechoslovakia).

Table 2 lists the synthesis conditions of the supported samples and their content of the VPO phase. It can be seen that the content of substance deposited onto the support surface, found by different methods is in satisfactory agreement. The amount of the VPO phase deposited onto the carbon surface is determined by several factors. In particular, the content of VPO on carbons with a large pore volume (both unoxidized and oxidized), namely, on A2PS and PS-3, is noticeably higher than that on KAU, whose pore volume is nearly

Table 3. Effect of the synthesis conditions on the crystal structure of the supported VHP phase

Support	Synthesis conditions		Caracteristics of VHP phase		
			I_{001}, a. u.	I_{001}/I_{220}	D_{001}, nm
Unoxidized A2PS	MWT	150	–	–	–
	MWT	175	5100	3.05	29.4
	HTT	150	–	–	–
	HTT	175	3700	2.80	29.0
	HTT	150	2000	1.10	28.5
Oxidized A2PS	MWT	175	2800	1.09	26.1
	HTT	175	1800	1.01	27.5
Unoxidized PS-3	MWT	175	2000	1.98	21.7
	HTT	175	2200	2.05	22.5
Oxidized PS-3	MWT	175	2800	1.32	25.2
	HTT	175	3500	1.10	26.7

two times smaller. In accordance with this circumstance, the surface concentration of the VPO phase formed from vanadium oxide is the lowest on samples of almost nonporous graphite. Another possible reason is that the graphite surface has the minimum amount of functional groups [18].

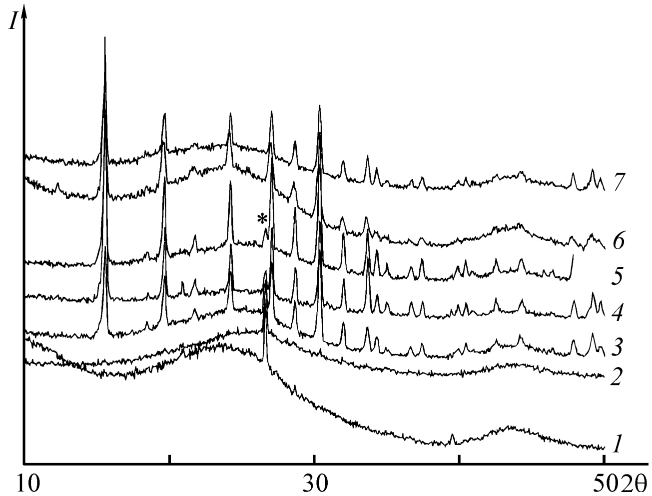

Fig. 1. X-ray diffraction patterns of (*1*) unoxidized A2PS carbon; (*2–5*) samples deposited from V_2O_5 on A2PS support: (*2*) unoxidized, HTT, 150°C; (*3*) oxidized, HTT, 150°C; (*4*) unoxidized, MWT, 175°C; (*5*) oxidized, MWT, 175°C; and (*6–7*) samples supported by PS-3: (*6*) unoxidized, MWT, 175°C; and (*7*) oxidized, MWT, 175°C. (*I*) Intensity and (2θ) Bragg angle; the same for Figs. 2 and 3.

The oxidation of carbons leads to an increase in the degree of deposition of the VPO phase (for graphite, the degree of deposition grows insignificantly), although the severe oxidation conditions (high temperature, concentrated H_2O_2, double oxidation) affect the formation of the VPO phase on the host surface in the opposite way. This can be seen by the example of KAU and will be discussed in more detail below. It can also be seen that, with V_2O_5 contained in the reaction mixture, the amount of the supported substance is substantially larger than that in the case of the ammonium metavanadate solution. This is primarily due to the low solubility of NH_4VO_3 in water (even at elevated temperatures). An increase in the content of the supported VPO is also favored by elevating the temperature of the deposition reaction and by using MWT, instead of HTT, despite the substantially shorter duration of the first kind of treatment.

The X-ray diffraction pattern of the unoxidized and oxidized A2PS (Fig. 1, curve *1*) contains, similarly for all carbons, two halos and a rather high-intensity reflection at 2θ = 26.6°, which apparently belongs to impurities (the position of this peak is denoted by symbol “*,” curve *5*). An amorphous (or X-ray-amorphous) VPO phase is formed on the surface of the unoxidized carbons A2PS and PS-3 from V_2O_5 by HTT and MWT at 150°C (curve *2*). On the oxidized surface, a fairly well-crystallized VHP phase is formed in accordance with Eq. (1), with the intensity ratio of the reflections from the basal (001) and lateral (220) planes, I_{001}/I_{220}, being close to unity:

$$V_2O_5 + 2H_3PO_4 = 2VOHPO_4 \cdot 0.5H_2O + H_2O + 0.5O_2. \quad (1)$$

The value of I_{001}/I_{220} is important because it determines the possible pathway of catalytic reactions: partial oxidation of hydrocarbons occurs on the basal plane, and their oxidative dehydrogenation, on the lateral surface [2]. Raising the temperature at which the deposition reaction is performed to 175°C favors VHP formation even on the surface of the starting (unoxidized) carbons (curve *4*).

If the degree of crystallinity of this phase is judged from the absolute intensities of reflections from the (001) and (220) planes (I_{001} and I_{220}) and from the crystallite sizes in the (001) plane (D_{001}), a conclusion can be made that the VHP obtained at 175°C on oxidized samples has a less perfect crystal structure than that produced at the same temperature on unoxidized A2PS (Table 3).

On passing from the unoxidized support to that subjected to oxidation, the I_{001}/I_{220} for the supported VHP phase sharply decreases. For example, this ratio for samples prepared on unoxidized A2PS by MWT and HTT is 3.05 and 2.80, respectively. An VHP phase with $I_{001}/I_{220} \approx 1$ is formed on the oxidized surface. It should also be noted that, as the deposition temperature is raised, and also as a consequence of the oxidation of the support, the intensity of the impurity line of A2PS substantially decreases and the halos characteristic of the carbons almost disappear, which may indicate that the surface layer of the carbon is transformed.

Similar X-ray diffraction data were obtained for samples synthesized by the HTT and MWT techniques on PS-3 carbon (Fig. 1, curves *6* and *7*): at 175°C, almost pure (without other crystalline phases) VHP is formed on both the unoxidized and oxidized carbon. As also for A2PS carbon, the value of I_{001}/I_{220} is smaller in this case for VHP deposited onto oxidized carbon, compared with VHP prepared on unoxidized PS-3.

Interesting results were obtained for samples deposited from the ammonium metavanadate solution onto the surface of A2PS. On the one hand, the low solubility of this salt in water makes reasonable the lower concentration of the supported phase (Table 2).

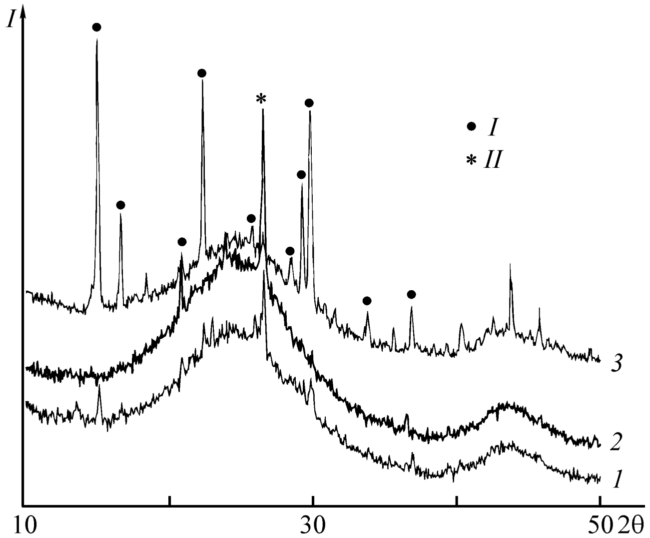

Fig. 2. X-ray diffraction patterns of samples deposited from NH_4VO_3 at 175°C onto A2PS support: (*1*) unoxidized, MWT; (*2*) unoxidized, HTT; and (*3*) oxidized, HTT. (*I*) Principal reflections of NH_4VO_3 and (*II*) reflection of an impurity.

On the other hand, according to DTA, the combustion of carbon in these samples begins at a higher temperature than that for composites synthesized from V_2O_5 (Table 2). This may occur because, in deposition from an NH_4VO_3 solution, the VPO phase more uniformly covers the carbon surface and thereby more strongly shields it from the access of atmospheric oxygen under heating. As evidence in favor of this assumption serves the fact that the degree of deposition on the oxidized surface is higher, and the onset temperature of carbon combustion is also higher: 480°C against 420°C for a sample prepared on the unoxidized A2PS. XPA data indicate that a mixed ammonium and vanadium(3+) phosphate $NH_4VP_2O_7$ is formed on the surface of A2PS carbon by the reaction

$$NH_4VO_3 + 2H_3PO_4 = NH_4VP_2O_7 + 3H_2O + 0.5O_2. \quad (2)$$

On the oxidized carbon, the intensity of lines of this phase is rather high and substantially exceeds that for the sample prepared on the unoxidized sample (Fig. 2). The crystallite size calculated in the plane corresponding to the strongest reflection at 2θ = 15.1° somewhat increases on passing from unoxidized A2PS to that subjected to oxidation, from 22.9 to 24.1 nm. The deep reduction of vanadium, compared with the case of deposition from V_2O_5, may be due to a larger area of the surface of interaction between reagents in the case of a solution, compared with the contact of solid phases (V_2O_5 and carbon). The DTA curves of

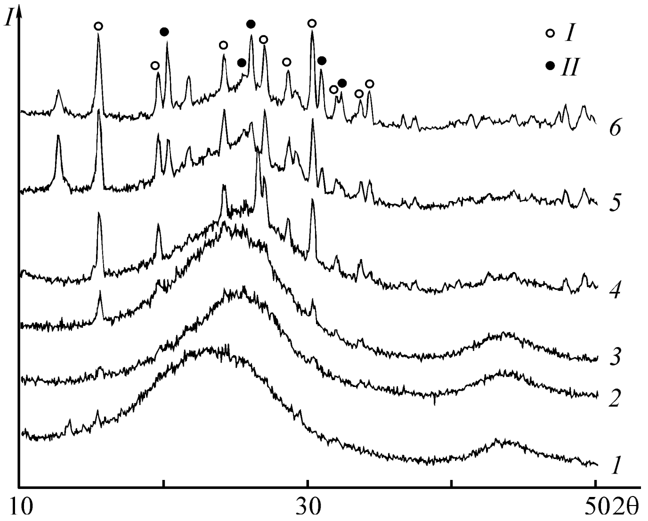

Fig. 3. X-ray diffraction patterns of (*1*) unoxidized KAU carbon; (*2*–*5*) samples deposited at 175°C onto KAU: (*2*) unoxidized, (*3*) once oxidized with 30% H_2O_2, (*4*) twice oxidized with a single deposition, (*5*) twice oxidized with two depositions; and (*6*) VPO sample. Reflections: (*I*) VHP and (*II*) V_2O_5.

these samples show two exothermic effects peaked at 500–535 and 800°C, which can be attributed to carbon combustion and disintegration of the double pyrophosphate. Thus, this compound is highly thermally stable in the supported state. It should be noted that this phase of mixed pyrophosphate of ammonium and triply charged vanadium is a catalyst for oxidative ammonolysis of hydrocarbons [19].

Figure 3 shows X-ray diffraction patterns, and Table 4 lists some parameters of samples synthesized from V_2O_5 on the surface of KAU. It can be seen that a VHP phase with several low-intensity, on the background of a halo, reflections is formed on the unoxidized and once-oxidized KAU, with the I_{001}/I_{220} ratio close to unity. After a single deposition onto twice oxidized carbon, all lines characteristic of VHP are seen in the X-ray diffraction pattern and their intensity increases (Table 4). No reflections associated with V_2O_5 are observed in these diffraction patterns. At the same time, another pattern is observed for a sample prepared by double deposition of VPO onto a twice oxidized KAU, as well as for a sample produced by single deposition of VPO onto a carbon oxidized with 50% H_2O_2. A specific feature of these samples is that their X-ray diffraction patterns contain, in addition to VHP reflections, peaks of *V*/*P* micas (V^{4+}–V^{5+} phosphates) at 2θ 12.71, 20.20, and 29.13° and of the starting V_2O_5. Consequently, in a repeated deposition onto a twice oxidized carbon, the amount of centers that can reduce V^{5+} to V^{4+} on the surface is insufficient. Similarly, reduction of the whole amount of V_2O_{-5} in deposition of VPO onto a KAU treated with 50% H_2O_2, i.e., onto a strongly oxidized surface, is apparently also impossible.

Thus, it can be assumed that, for making larger the amount of the VPO phase deposited from V_2O_5, a certain optimal content of oxygen containing groups on the carbon surface (optimal degree of oxidation of the surface) is required. Consequently, it is necessary to perform the HTT or MWT of carbons with 30% H_2O_2 at a comparatively low temperature, e.g., at 200°C, which was demonstrated for the example of A2PS and PS-3 carbons.

An additional specific feature observed in VPO deposition onto oxidized KAU is demonstrated by comparison of XPA data for supported and bulk VPO samples (the latter were isolated from the reaction mixture after 5 h of treatment). For example, the bulk sample formed in deposition onto a twice oxidized carbon is a pure well-crystallized VHP phase with

Table 4. Effect of the synthesis conditions of samples supported by KAU carbon on their crystal and pores structure

Support	Parameters of the VHP phase			S_{BET}, m^2 g^{-1}	V_{N_2}, cm^3 g^{-1}
	I_{001}, a. u.	I_{001}/I_{220}	D_{001}, nm		
Unoxidized KAU	200	1.1	19.9	770	0.32
Oxidized KAU, 350°C 30% H_2O_2	400	1.0	19.0	722	0.35
Twice oxidized KAU, 350°C 30% H_2O_2	800	0.9	17.0	480	0.34
	1000	1.0	18.4	340	0.30
Oxidized KAU, 350°C 50% H_2O_2	1000	1.0	19.1	347	0.20

I_{001}/I_{220} = 3.5, I_{001} = 10500 a. u., and crystallite size D_{001} = 23.3 nm. At the same time, the final product of the deposition reaction (Fig. 3, X-ray diffraction pattern 5) has the following parameters: I_{001} = 1100 a. u., I_{001}/I_{220} = 1.0, and D_{001} = 18.4 nm. Thus, it can be concluded that the crystallographic planes of VHP are reoriented upon deposition of this phase onto the surface of oxidized carbon and its crystallites are dispersed to a certain extent.

In hydrothermal deposition of VPO onto unoxidized and oxidized nonporous carbon nanotubes with the use of V_2O_5 at 170°C, the vanadyl dihydrophosphate phase with $P/V = 2$ is formed; raising the temperature to 200°C favors formation of VHP ($P/V = 1$). The crystallite size of these phases is 5–10 nm, and I_{001}/I_{220} = 2.5–2.7. Hydrothermal and microwave deposition from V_2O_5 and NH_4VO_3 onto the surface of porous C–NT yields the VHP and $NH_4VP_2O_7$ phases, respectively, as observed for A2PS carbon.

The porosity parameters calculated from nitrogen adsorption isotherms are listed in Table 4 for KAU-based samples and in Table 5 for those on A2PS and PS-3 carbons. The trends in the change in the adsorption-structural parameters are the same for all the composites obtained on both unoxidized and oxidized carbons. Because pores (primarily micropores) are filled in deposition of the VPO phase onto carbons and the surface is blocked, the specific surface area and the volume of all kinds of pores decrease, which can be seen from the data in Table 5 for samples on A2PS and PS-3. For nearly all of the samples studied these changes correlate with the content of the VPO phase in a supported sample. As a rule, the surface area and volume of pores change to a greater extent in the course of MWT. Another trend consists in that V_{N2} and V_{mi} decrease more strongly upon deposition onto an unoxidized carbon. The same trends are observed for samples supported by KAU (Table 4) and porous carbon nanotubes. In the case of nonporous C–NT, the pores structure of supported samples is formed in the course of the deposition process itself (or in preliminary oxidation). For example, the deposition onto unoxidized nonporous C-NT gives composites with a specific surface area of 35–45 $m^2 g^{-1}$ and total pore volume of 1.0–1.4 $cm^3 g^{-1}$, whereas on oxidized nanotubes, samples with a weakly developed porous structure are formed, with a specific surface area of 10–15 $m^2 g^{-1}$ and pore volume of less than 0.1 $cm^3 g^{-1}$.

Figure 4 shows SEM micrographs characterizing the surface morphology of supported samples. Analysis of these images suggests the following. First, the coating on the carbon surface is not continuous, with separate crystallites of the VPO phase or

Table 5. Parameters of the pores structure of VPO samples supported by A2PS, PS-3, and C–NT carbons

Support	Synthesis conditions		S_{BET}, $m^2 g^{-1}$	S_{m_i}, $m^2 g^{-1}$	V_{N_2}, $cm^3 g^{-1}$	V_{m_i}, $cm^3 g^{-1}$	V_{m_e}, $cm^3 g^{-1}$
	HTT, MWT	T, °C					
Unoxidized A2PS	HTT	150	732	348	0.44	0.15	0.29
A2PS oxidized HTT 150	HTT	150	957	314	0.53	0.14	0.39
Unoxidized A2PS	HTT	175	845	364	0.49	0.16	0.33
Unoxidized A2PS	MWT	150	662	246	0.41	0.11	0.30
A2PS oxidized MWT 150	MWT	150	941	388	0.55	0.17	0.38
Unoxidized A2PS	MWT	175	1129	501	0.65	0.22	0.43
Unoxidized PS –3	HTT	175	1617	522	0.90	0.23	0.57
PS-3 oxidized HTT 175	HTT	175	1526	460	0.85	0.20	0.53
Unoxidized porous C-NT	HTT	175	165	20	0.62	0.01	0.61
Unoxidized porous C-NT	MWT	175	136	26	0.66	0.01	0.65

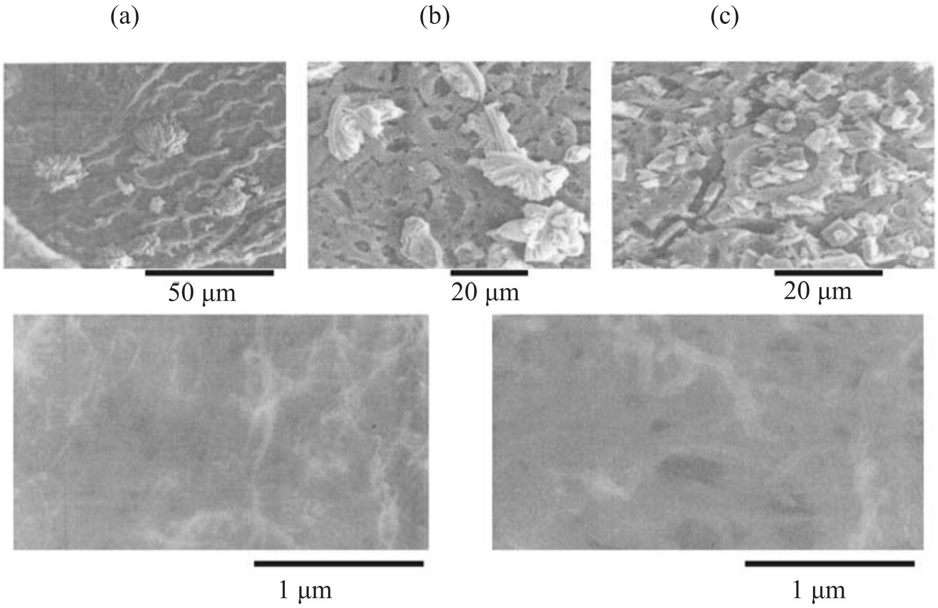

Fig. 4. SEM micrographs of samples deposited by HTT onto the surface of (a) unoxidized and (b) oxidized A2PS, (c) twice oxidized KAU, (d) unoxidized nonporous C–NT, and (e) supported VPO sample upon HTT at 200°C.

aggregates of these formed in the deposition process. Second, the coverage of the surface and the size and shape of VPO crystallites depend on the nature and porous structure of a support carbon and on the oxidation state of its surface. VPO crystals of cylindrical shape, 3–5 μm long and 0.5–1.0 μm in diameter, can be seen on the surface of unoxidized and oxidized KAU (Fig. 4c). On unoxidized A2Ps, crystallites of the same kind form 20-μm aggregates in the form of rosettes (Fig. 4b). On oxidized A2PS, the surface coverage by the VPO phase increases, with its aggregates formed as bundles of bent rods with a thickness of about 1 μm and length of 15–25 μm (Fig. 4a). It should be noted that these data for the morphology of supported VPO crystals differ from those for the bulk VHP, whose crystallites frequently have the form of small roses [7, 20]. It is also of interest that, with nonporous C-NT used as a support, the VPO phase is deposited onto the outer surface of nanotubes, with the result that their outer diameter increases from 40 to 60 nm (Figs. 4d, 4e).

The thermal stability of the VPO/carbon composites synthesized (which is important for their applicability as catalysts) was assessed using the DTA data. As it can be seen from the data in Table 2, carbon starts to be oxidized at 360–390°C for A2PS-supported samples and at 400–410°C for those on PS-3. For samples produced by deposition of ammonium metavanadate from solution, the onset of the carbon oxidation process is shifted to 420–480°C. The highest thermal stability is observed for composites produced on graphite and carbon nanotubes, which is in good agreement with the properties of this kind of materials. For VPO/graphite samples deposited from V_2O_5, the combustion onsets at 460–465°C. The composites on C–NT are oxidized at 520–900°C, with only apparently amorphous carbon, nearly always present in nanotubes of this kind, subjected to combustion [4, 15]. These results suggest that the composites obtained can be quite thermally stable in some catalytic processes (e.g., in oxidation of n-butane to maleic anhydride and in ammoxidation of organic compounds; and composites based on nanotubes and graphite, also in oxidative dehydrogenation of hydrocarbons).

CONCLUSIONS

(1) Hydrothermal and microwave deposition of vanadium phosphates onto various unoxidized and oxidized carbon materials yields, depending on a source of vanadium, composites constituted by vanadyl hydrophosphate + carbon support and mixed vanadium(3+)-ammonium phosphate + carbon support. The composites have controllable characteristics of the crystal and porous structure and varied thermal stability and surface morphology.

(2) Preliminary oxidation of carbon materials under the optimal conditions (200°C, 30% hydrogen per-

oxide) leads to an increase in the concentration of the supported VPO phase and to a change in its crystallographic parameters.

REFERENCES

1. Stailz, E.B., *Nositeli i nanesennye katalizatory* (Supports and Supported Catalysts), Moscow: Khimia, 1980.
2. Krylov, O.V., *Geterogennyi kataliz* (Heterogeneous Catalysis), Moscow: Akademkniga, 2004.
3. Ryashentseva, M.A., Egorov, E.V., Trusov, A.I., et al., *Usp. Khim*., 2006, vol.. 75, no. 11, p. 1119.
4. Fenelonov, V.B., *Poristyi uglerod* (Porous Carbon), Novosibirsk: Inst Kataliza Sib. Otd. Ross. Akad. Nauk, 1995.
5. Rodriguez-Reinoso, F., *Carbon*, 1998, vol. 36, p. 159.
6. Tarkovskaya, I.A., *Okislennyi ugol’* (Oxidized Carbon), Kiev: Naukova dumka, 1981.
7. Hutchings, G.J., *J. Mater. Chem*., 2004, vol. 14, p. 3385.
8. Clearfield, A., *Ann. Rev. Mater*., 1984, vol. 14, no. 2, p. 205.
9. *Inorganic Phosphate Materials*, Kanazawa, T., Ed., Amsterdam: Elsevier, 1989.
10. Dupre, N., Wallez, G., Gaubicher, J., and Quarton, N., *J. Solid State Chem*., 2004, vol. 177, no. 12, p. 2896.
11. Sidorchuk, V.V., Skubishevska-Zemba, Ya., Khalameida, S.V., et al., *Zh. Prikl. Khim*., 2008, vol.. 81, no. 8, p. 1246.
12. Sidorchuk, V.V., *Neorg. Mater*., 1993, vol. 29, no. 2, p. 274.
13. Pillai, U.R., Sahle-Demessie, E., and Varma, R.S., *Appl. Catal. A*, 2003, vol. 252, p. 1.
14. Zeng, L., Jiang, H., and Niu, J., *J. Mol. Catal*., 2005, vol. 232, p. 119.
15. Melezhik, A.V., Sementsov, Yu.I., and Yanchenko, V.V., *Zh. Prikl. Khim*., 2005, vol.. 78, no. 6, pp. 938.
16. Sidorchuk, V.V., *Zh. Prikl. Khim*., 2006, vol.. 79, no. 9, p. 1444.
17. Gregg, S.J. and Sing, K.S.W., *Adsorption, Surface Area and Porosity*, London: Academic Press, 1982.
18. Chernysh, I.G., Karpov, I.I., Prikhod’ko, G.P., and Shai, V.M., *Fiziko-khimicheskie svoistva grafita i ego soedinenii* (Physicochemical Properties of Graphite and Its Compounds), Kiev: Naukova dumka, 1990.
19. Martin, A., Steinike, U., Rabe, S., et al., *J. Chem. Soc., Faraday Trans*., 1997, vol. 93, no. 21, p. 3855.
20. Tauffiq-Yap, Y.H., Leong, L.K., Hussein, M.Z., et al., *Catal. Today*, 2004, vols. 93–95, pp. 715.